

Perspective

Development status of electrocatalytic hydrogenation of biomass small molecules and prospects for industrial production

Yuchen Lei,^{1,3} Fuhai Zhang,^{2,3} Wenbin Zhang,¹ and Wei Zhao^{1,*}¹Institute for Advanced Study, Shenzhen University, Shenzhen, Guangdong 518060, China²Department of Chemistry, Colgate University, 13 Oak Drive, Hamilton, NY 13346, United States³These authors contributed equally*Correspondence: weizhao@szu.edu.cn<https://doi.org/10.1016/j.isci.2025.111908>

SUMMARY

Biomass is the only renewable organic carbon resource in nature, and utilization of biomass is important for carbon neutrality. Currently, depolymerizing biomass macromolecules into small organic monomers via thermocatalytic pyrolysis is a well-established technique. Further valorization of these biomass small molecules to value-added products has attracted increasing attention, especially via electrochemistry coupling green electricity. Electrocatalytic hydrogenation (ECH) directly uses hydrogen from water and operates under mild conditions (e.g., ambient temperature and pressure), which plays an important role for upgrading biomass small molecules and avoids substantial CO₂ emission. In this review, we will provide a summary of recent achievements in ECH of biomass small molecules, with a review focus on the research about pushing ECH toward industrial-scale productivities. We will also discuss the existing problems and challenges in this field and propose an outlook for the future developments.

INTRODUCTION

The widespread utilization of petrochemical feedstocks, contributing to greenhouse effect, makes energy conservation, emission reduction, and sustainable development dominant topics. As the cost of renewable electricity decreases, there is growing interest in seeking alternatives to fossil resources with electricity. In contemporary efforts to reduce greenhouse gas emissions, advancing and applying bioenergy is critical for developing clean energy and pursuing carbon neutrality.^{1–3} Biomass stands out due to its abundance, cost-effectiveness, and environmental friendliness, coupled with a substantial capacity for use, making it a critical component of future energy supplies.^{4,5} Valorizing biomass small molecules into high value organic chemicals offers a promising alternative to fossil resources. For example, 5-hydroxymethylfurfural (HMF), derived from lignocellulose biomass, serves as a widely used industrial organic substrate. HMF can be selectively hydrogenated into 2,5-bis(hydroxymethyl)furan (BHMF), a robust bio-derived diol used as a monomer in biomaterials and fuel production.⁶ Similarly, guaiacol, a prototypical aromatic monomer derived from lignin biomass, can be electrocatalytically reduced to 2-methoxy-cyclohexanol (2MC), an intermediate in producing high-value β-lactam antibiotics for treating human immunodeficiency viruses.^{7,8}

Biomass small molecules valorization primarily employs biochemical and thermochemical processes.⁹ Biochemical processes offer superior product selectivity but suffer from slow reaction kinetics and strict feedstock requirements.¹⁰ Although

thermochemical processes can expedite biomass small molecules conversion into solid (biochar), liquid (bio-oil), and gaseous products (e.g., CO and H₂), they often involve significant drawbacks. Thermocatalytic hydrogenation (TCH), in particular, generally associates with high hydrogen pressure and reaction temperature (150°C–400°C and 0.5–20 MPa H₂ pressures).^{11,12} And the experimental conditions employed for TCH can lead to catalyst deactivation due to coking, poisoning, or sintering issues.¹³ Additionally, the hydrogen produced during TCH processes will lead to substantial CO₂ emission.¹⁴

Recent years have seen a significant reduction in the cost of renewable electricity,¹⁵ sparking increased interest in applying electrochemical processes to biomass small molecules valorization. Electrocatalytic hydrogenation (ECH) is regarded as an environmentally sustainable route with several advantages: (1) the ECH can be powered by intermittent energy sources, such as solar energy; (2) the hydrogen source is water instead of H₂, bypassing the cost and transportation for hydrogen; and (3) the process operates under mild conditions, avoiding the high heat expenses required for TCH and severe polymerization of biomass.^{12,16–21} Although there have been significant advancements in ECH process, it still faces challenges in achieving industrial production due to the competition of hydrogen evolution reaction (HER) and the insufficient economic value of conversion process. At large current densities, the rate of ECH will get improved. However, concurrently, the competition of HER intensifies, which limits the yield of target products.^{22,23} And the selection of target product will affect profitability. For example, when guaiacol is



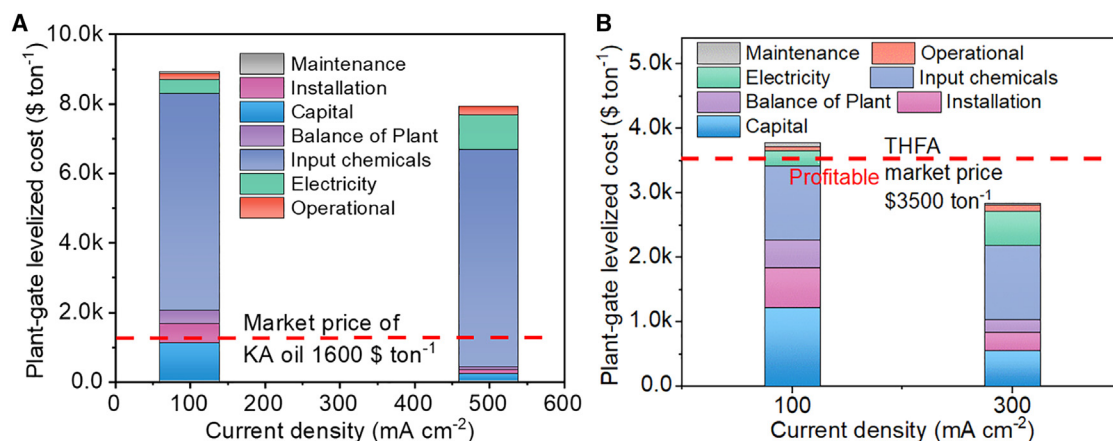


Figure 1. Technoeconomic analysis breakdown costs for different biomass small molecules at various current densities

(A) KA oil from ECH of guaiacol.

(B) Tetrahydrofurfuryl alcohol (THFA) from ECH of furfural alcohol (FA). Reprinted with permission from Peng et al.²⁴ Copyright 2023 Springer Nature.

hydrogenated to produce KA oil (\$1600 ton⁻¹), the entire process fails to achieve profitability even at 500 mA cm⁻² (Figure 1A).²⁴ Consequently, the focus should be shifted to the production of higher-value products. Achieving industrial-scale productivities requires operating at larger current densities while maintaining reasonable FEs. Swift and effective conversion can lower capital costs per unit of products associated with electrolyzer surface area and improve economic efficiency (Figure 1B), which is critical for the commercialization and sustainable development of biomass small molecules valorization technology.²⁵

Up to now, many reviews have discussed the electrocatalytic conversion of biomass for upgrading, but lacked of discussions about industrial-relevant current densities production. This review focus on how the engineering of electrolyzers improve the ECH of biomass small molecules and aims to present detailed discussions on design of ECH electrolyzers, electrode surface area, catalyst design, and selection of electrolyte to advance ECH toward achieving industrial current density. Additionally, the current issues and challenges within this field will be investigated, and insights will be provided for the future developments toward industrial production (Figure 2).

ENGINEERING OF ECH ELECTROLYZERS

The electrocatalytic performance is primarily evaluated by the FE, which quantifies the effectiveness of charge (electrons) transfer in a system, enabling the electrocatalytic reaction toward the desired products. Additionally, the current density is a critical metric. Achieving both high FE and large current density are imperative for the industrial application of electrocatalysis. H-cell and flow cell configurations, along with the membrane electrode assembly (MEA) based flow cell, are utilized electrochemical electrolyzers for the ECH of biomass small molecules.

Undivided cell

Undivided cells are traditional electrolyzer that features working electrode, reference electrode, and counter electrode within one single chamber. Owing to its straightforward, the undivided cells

have been widely used within the field of electrochemistry. For example, Prof. Weix's group reported a nickel-catalyzed reductive cross-electrophile coupling reaction in acetonitrile, employing diisopropylethylamine as the terminal reductant within an undivided cell. This approach avoids the use of metal reductants and amide solvents.²⁶ Mei et al. reported an example of a Ni-catalyzed electrochemical enantioselective reductive homocoupling of aryl bromides, utilizing chiral pyridine-oxazoline ligands. This approach makes biaryls a good yield and enantioselectivity with an undivided cell.²⁷ Nobe et al. employed an undivided packed-bed reactor to simultaneously oxidize glucose to gluconic acid and reduce it to sorbitol. Utilizing a Raney Ni powder cathode in conjunction with a graphite chip anode, they achieved a glucose conversion rate of 28% and a current efficiency of up to 100%.²⁸ However, in contrast to undivided cells, divided cells, separated by a suitable membrane, can prevent substrates and target products from being oxidized at the anode electrode.¹² Therefore, the divided cells are more widely applied in the ECH of biomass small molecules.

H-cell

In a standard H-cell configuration, the working and reference electrodes are situated within the cathode compartment, where the ECH of biomass small molecules takes place at the cathode. Concurrently, the oxygen evolution reaction (OER) occurs at the anode. The counter electrode is located within the anode compartment. The cathode and anode sections are divided by an ion exchange membrane and are filled with the respective electrolytes (Figure 3A).^{29–33} The straightforward configuration of H-cell allows for rapid evaluation of catalysts and operational conditions.³⁴ Catalysts can be coated onto a substrate (e.g., carbon felt) and fixed using an electrode clamp to ensure an adequate exposed area. Various deposition techniques including electrodeposition, impregnation, and hydrothermal can be employed to fabricate the working electrode.^{35–40} Some catalysts with superior activity for the ECH of biomass small molecules catalysts have been shown in H-cells.^{41–45} For example, Zhao et al. loaded the metallic Pd on carbon felt

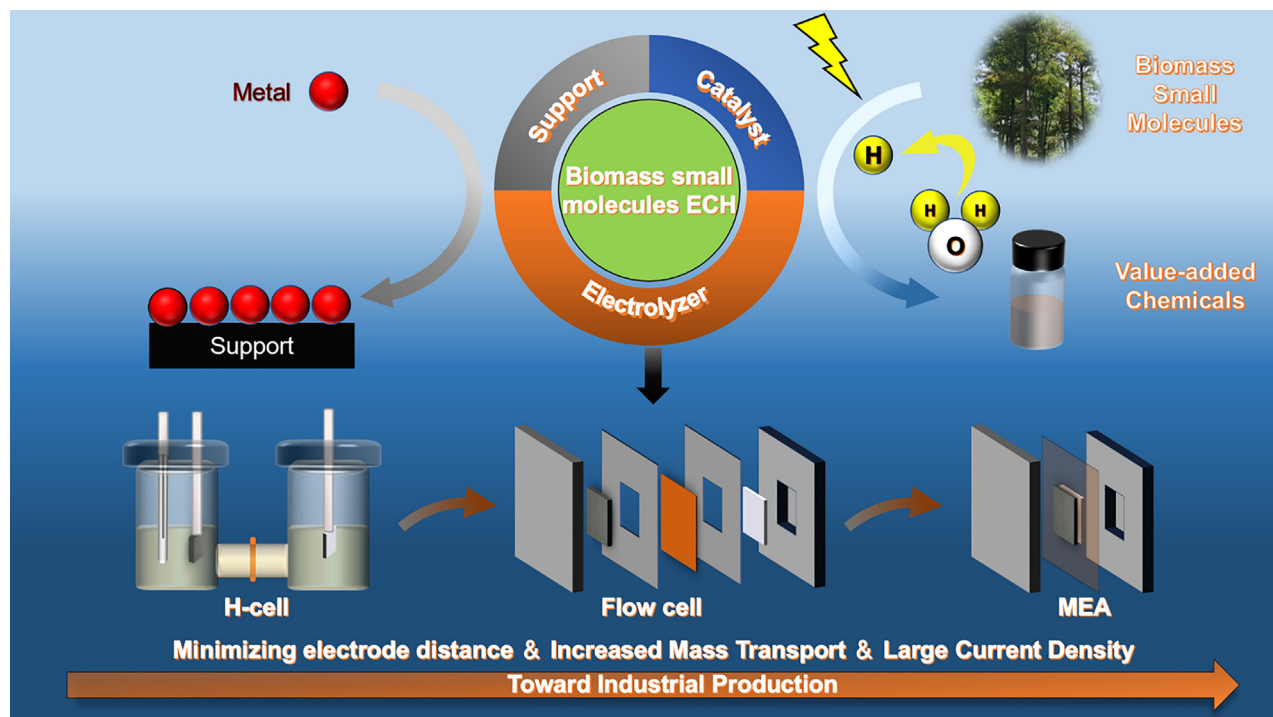


Figure 2. Schematic diagram of the topics covered in this review

(Pd/CF) for the ECH of cinnamaldehyde. The Pd/CF achieved a total FE of 87.54%, a partial FE of 41.15% for the main product cinnamic alcohol, and stability of 23 h at 50 mA cm^{-2} .⁴¹ Duan et al. constructed Ru₁Cu Single-atom catalysts (SACs) by dispersing isolated Ru atoms on Cu nanowires. The Ru₁Cu SACs exhibited an ECH of HMF to BHM with an FE of $\sim 85.6\%$ and stability of $\sim 4 \text{ h}$ at $\sim 42 \text{ mA cm}^{-2}$.⁴²

However, the industrial application of H-cell is limited by several reasons. First, the reactions and pathways involved in the ECH of biomass small molecules are acutely dependent on the local microenvironment, which affects the energetics of the reactions taking place on a catalyst's surface.^{50,51} Since the local microenvironment is altered by variations in current density and applied potential, the results from H-cells are not entirely applicable to industrial settings. Second, in most H-cells, the relatively large distance between the anode and the cathode, along with the associated resistance to ion transport, leads to significant voltage losses. Third, unsaturated substrates must diffuse considerable distances to reach the electrode pores where the metal catalyst is deposited, which is necessary for initiating the reaction. Although 3D porous electrodes offer a substantial surface area for ECH, mass transport limitations and kinetic diffusion still significantly constrain the reaction rate.

To address the aforementioned challenges, certain measures have been implemented to modify the H-cell. For minimizing internal Ohmic resistance, an improved H-cell with a short distance between the electrodes and the membrane was implemented (Figure 3B).⁴⁶ As for the mass transport in the H-cell, some researchers have attempted to modify the catalyst types, suspending catalysts in the electrolyte.^{47,48,52,53} For example,

Gyenge et al. investigated ECH of guaiacol using a membrane-divided stirred slurry electrochemical reactor (SSER) configuration with a dispersed catalyst Pt/C in the cathode compartment (Figure 3C). Their experiments demonstrated that the reactor can be efficiently operated at current density ranging from 109 to 225 mA cm^{-2} with an FE up to 48%.⁴⁷ Deng et al. developed a dual-catalyst electrochemical method that achieved a high FE over 99% for various chemicals and a large current density at 800 mA cm^{-2} in the ECH of model bio-oil compounds, phenol and guaiacol (Figure 3D). The dual-catalyst system consists of suspended catalyst particles and a soluble polyoxometalate (POM) that serves as an electron transfer (ET) catalyst. Since the Pt catalyst is dispersed in the solution, the diffusion and collision of reactant molecules with the catalyst surface are significantly enhanced, enabling both high FE and large current density to be attained concurrently.⁴⁸ However, the development of the SSER system is hindered by several challenges, including the erosion of catalyst caused by intense particles friction, the non-uniform polarization of the electrocatalyst bed due to loss of electric contact, and the requirement to separate and recover the catalyst from the liquid product. Meanwhile, the dual-catalyst system employs a considerable amount of catalysts to achieve high FE and large current densities when compared with conventional ECH systems, which is a factor that must be considered for industrial production when compared to conventional ECH systems.⁵⁴ The existing researches have yet to offer effective solutions to these challenges, necessitating further investigation in the future. For the ECH reactions occur at potentials much more negative than the HER, indicating H₂ formation is more thermodynamically favored, a membrane reactor was utilized.

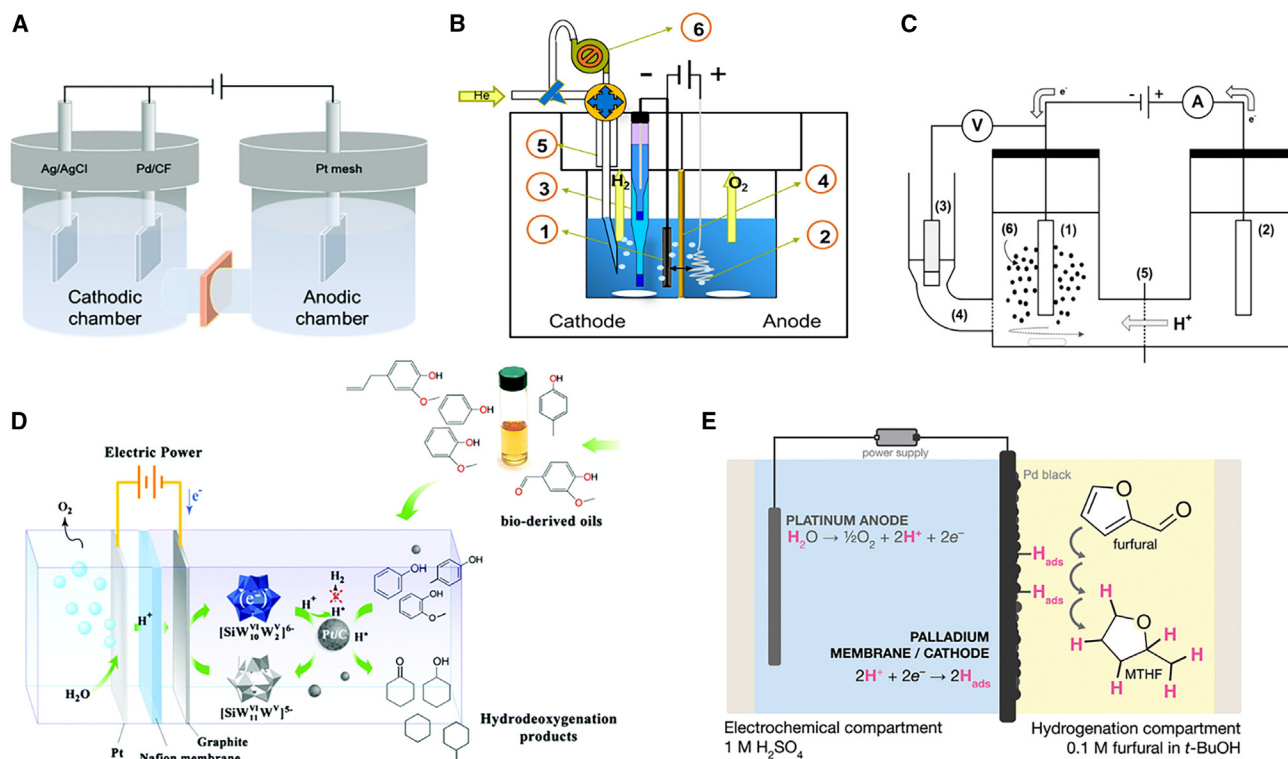


Figure 3. The schematic illustrating of the H-cell based electrolyzer system

(A) H-cell reactor. Reprinted with permission from Chen et al.⁴¹ Copyright 2022 Royal Society of Chemistry.

(B) Improved H-cell reactor. Reprinted with permission from Song et al.⁴⁶ Copyright 2016 Elsevier.

(C) Stirred slurry electrochemical reactor (SSEr) with suspending Pt/C. Reprinted with permission from Wijaya et al.⁴⁷ Copyright 2019 John Wiley and Sons.

(D) POM-Pt/C dual-catalyst system. Reprinted with permission from Liu et al.⁴⁸ Copyright 2020 Royal Society of Chemistry.

(E) Palladium membrane reactor. Reprinted with permission from Stankovic et al.⁴⁹ Copyright 2023 Royal Society of Chemistry.

Within this H-cell based configuration, the site of water electrolysis is isolated from the site of hydrogenation (Figure 3E). Protons and hydrides were produced in an aqueous environment, with the ECH taking place in a neighboring compartment using organic solvents. The membrane reactor achieved the ECH of furfural (FF) to methyltetrahydrofuran with a selectivity of >75% at 200 mA cm⁻².⁴⁹

Flow cell

Despite many attempts and the realization of good performances, the intrinsic properties of the H-cell render it less than ideal for large-scale industrial applications. In industrial settings, there is a higher requirement for the stability, with continuous-flow reactor typically being favored over a batch process system.¹² In a complete experimental process, H-cell would prefer be used to explore the conditions at the beginning of ECH experiment design, which demonstrate the availability for further development.⁵⁵

As a continuous reactor, in a flow cell, the catholyte and anolyte are constantly pumped into the cathode and anode chambers, respectively, which promotes the diffusion of biomass molecules to the electrode surface, while minimizing mass transfer restrictions caused by hydrogen bubble interference at the electrode surface.⁵⁶ An ion exchange membrane separates the cathode and anode compartments to reduce crossover and prevent

product oxidation (Figure 4A). In contrast to the H-cell, the shortened distance between the electrodes, coupled with the improved mass transfer efficiency, results in decreased Ohmic resistance and increased reaction rate, showing the potential for industrial-scale ECH of biomass small molecules (Figure 4B). For example, Zhao et al. used the ternary PtRhAu catalysts for the ECH of guaiaacol. During the experiment, the metals were loaded onto CF, which is composed of abundant carbon fibers. The properties of high conductivity, large specific surface area, robust chemical stability, and enhanced mass transfer make CF an excellent support material. Coupled with the application of flow cell, the PtRhAu achieved a 58% FE toward 2-methoxycyclohexanol and maintained stability for 60 h at 200 mA cm⁻².⁸ And these modified characteristics can effectively relieve heat release from configuration and reduce the full-cell voltage during production (Figure 4C).²⁴

However, the increased resistance caused by the liquid electrolytes between the cathode and the anode in flow cells reduces the energy efficiency of the systems. The prospect of markedly decreasing internal resistance through the removal of the liquid electrolyte layer between the electrodes holds great promise. This advancement facilitates a higher current density and a lower cell voltage, which is in harmony with the demands of industrial usage. The MEA, commonly known as the zero-gap electrolysis

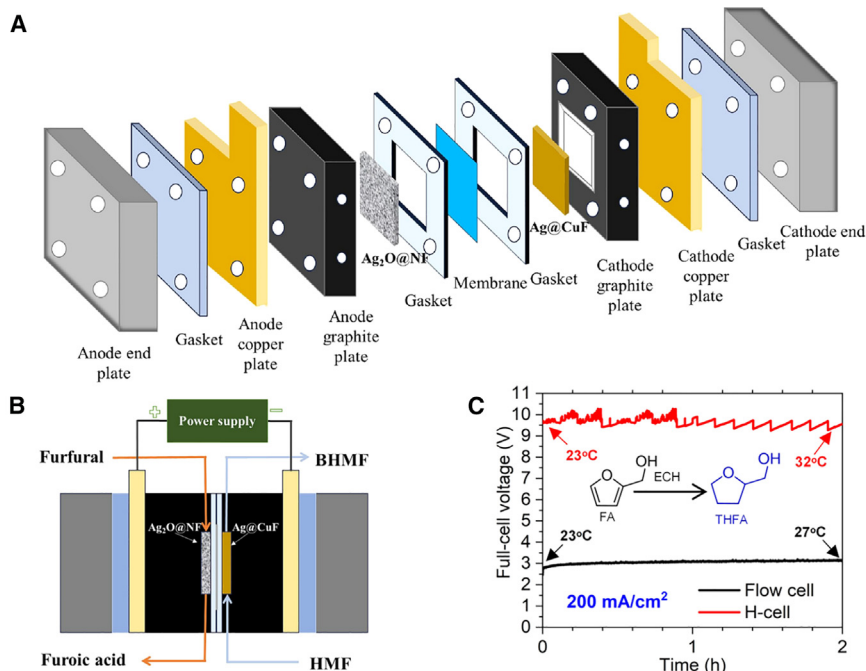


Figure 4. The schematic illustrating of the flow cell and comparison compared to H-cell

(A-B) Schematic of flow cell. Reprinted with permission from Dai et al.⁵⁵ Copyright 2024 Elsevier.

(C) Comparison of flow-cell and H-cell at 200 mA cm⁻² for 2 h continuous reaction. Reprinted with permission from Peng et al.²⁴ Copyright 2023 Springer Nature.

Product separation cost + other operational cost (10% of the electricity cost), (6) Electricity cost: Full-cell potential, FE, and electricity price, and (7) Input chemical cost: Reactant cost + electrolyte cost.²⁴

The capital cost is composed of electrolyzer, catalyst, membrane, and electrolyte. The capital cost per unit of product is related to the geometric area of electrode. When the current density is constant, the capital cost is in direct proportion to the increase of geometric area

cell, has a sandwich-like structure (Figure 5).^{57–59} The cathode layer, ion exchange membrane, and anode layer are tightly integrated, minimizing Ohmic resistance and cell potentials. Due to this design and the resulting decreased Ohmic losses, MEA-based cells enable higher current density, lower cell potential and improved energy efficiency. For example, Zhao et al. used an MEA of flow cell configuration with a Rh/CF working electrode to hydrogenate aromatic monomers derived from lignocellulose into high-value chemicals, achieving an FE up to 64% at industrial-scale current densities of 300–500 mA cm⁻². The Rh/CF sustained an FE over 56% at 300 mA cm⁻² during a 32 h continuous operation for transforming guaiacol into the desired product.²⁴ MEA electrolyzers outperform flow cells and H-cells in terms of energy efficiency, which enhances their appeal for industrial production. Herein, we summarized the ECH of various biomass in different electrolyzer systems in Table 1 for a more comprehensive performance comparison.

TECHNOECONOMIC ANALYSIS

Technoeconomic analysis (TEA), an economic-technical assessment, evaluates the viability of process and technology for commercial application from technical and economic perspectives. TEA concentrates not only on the performance of technology, but also on cost and market prospects. The TEA is mainly composed of the following aspects: (1) Capital cost: Electrolyzer cost + catalyst cost + membrane cost (5% of the electrolyzer) + electrolyte cost, (2) Installation cost: Lang factor (50%) × (electrolyzer cost + catalyst cost + membrane cost), (3) Maintenance cost: Maintenance frequency (1/day) × maintenance factor (5%) × (electrolyzer cost + catalyst cost + membrane cost), (4) Balance of plant: Balance of plant factor (35%) × (electrolyzer cost + catalyst cost + membrane cost), (5) Operational cost:

of electrode with unchanged capital cost per unit of product. When keeping production scale constant, the current density is in inverse proportion to the geometric area of electrode. Thus, the increase of current density will lead to a reduction in the capital cost per unit of product and lower the plant-gate levelized cost of the product. The high capital cost, attributed to electrolyzer and precious metal catalyst, can be reduced by increasing the current density. That is why the current density is crucial in determining the profitability of ECH and why a large current density is required for industrial-scale production. Current density, FE, and full-cell potential are the primary parameters influencing the plant-gate levelized cost of product. However, these three parameters are inherently interconnected, making it impractical to adjust one while keeping the others fixed. Optimally, ECH benefits from large current density, high FE and low full-cell potential. FE determines the selectivity of ECH and efficiency of energy utilization, and the full-cell potential is correlated with the electricity cost.

ACHIEVING INDUSTRIAL-SCALE CURRENT DENSITY

Industrial-scale current densities signify an increased electron transfer rate and chemical reaction rate, which accelerate the hydrogenation process of biomass small molecules. The capacity of processing bulk feedstocks is essential to achieve large-scale valorization of biomass small molecules. Furthermore, FE multiplied by total current density, which is partial current density, represents the real production rate of target products. The increase in current density results in a more negative applied potential and increased surface coverage of *H (adsorbed H), leading to the enhanced hydrogenation rate of biomass small molecules. However, on the other hand, HER will be also enhanced as the *H coverage increases. Furthermore, an

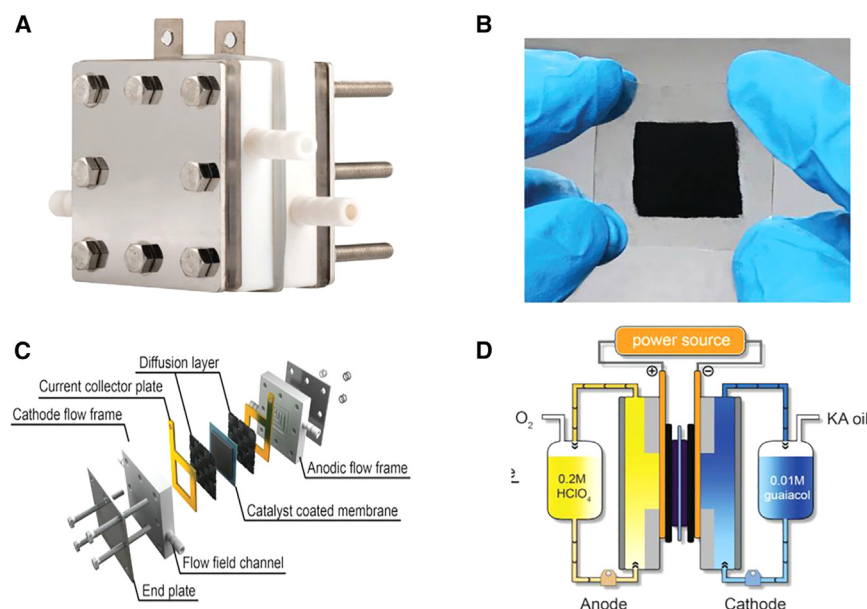


Figure 5. The schematic illustrating of the MEA based flow cell

(A) ECH electrolyzer cell.⁵⁹ (B) Catalyst-coated membrane in electrolyzer.⁵⁹ (C) The components of electrolyzer.⁵⁹ (D) Schematic of ECH reaction system.⁵⁹ Reprinted with permission from Zhou et al.⁵⁹ Copyright 2019 John Wiley and Sons.

increased generation of hydrogen gas bubbles from the catalyst surface obstruct the diffusion of biomass reactants and the adsorption of reactants on the catalyst, leading to a decline in FE. Moreover, given the multiple potential hydrogenation pathways in biomass small molecules, the final product distribution could be complex with various competing side-reactions.^{43,56} Thus, the key for industrial-scale ECH of biomass production is achieving large current densities with simultaneously maintaining relatively high FE for the target product. To realize that, we propose researchers can contribute from the following three aspects: novel and efficient electrode catalysts, new design of electrolyzer device, and new electrolytes specifically for electro-organic reactions.

Catalyst

A larger current density indicates a faster reaction rate, which is influenced by electronic and surface structures of the catalysts. Initially, the electronic effect, or the selection of electrocatalytic material, should be considered. Subsequently, the impact of the surface structure of the catalysts on the kinetics and mechanistic pathways of the electrocatalytic reaction, should be examined. The interaction between the catalyst and the reactant, governed by the catalyst's structure and composition, alters the reaction pathway.³⁵ The electron configuration and properties of the catalyst significantly impacts electrocatalytic activity.^{38,67,68} Catalysts predominantly feature transition metals possessing free d orbitals and unpaired d electrons. Chemisorption on transition metal catalysts' d orbitals activates molecules, lowering the activation energy and boosting electrocatalysis (e.g., Cu, Pd, Ru, Rh).^{29,36,41,58} Different catalysts in the same reaction system can alter adsorption free energies, influencing the reaction rate. An optimal catalyst binds adsorption intermediates with moderate strength, as binding that is too weak or strong is detrimental.^{11,12} Alloying and surface modification can adjust the adsorption free energies.²² Binary or ternary noble metal nanocomposite structures

exhibit the unique properties of their constituents plus synergistic effects from heteroatoms. Manipulating alloy composition and structure enhances physical and chemical properties for optimal performance.^{8,33,69}

The catalytic activity varies for the same catalyst with different structures due to distinct surface geometries.⁴⁴ The impact of surface structure on electrocatalysis is based on two main factors. First, the performance of catalysts depends on its surface chemical structure (composition and valence), geometric morphology, atomic

arrangement and electronic structure.^{31,39,59} Second, almost all ECH reactions are highly sensitive to surface structure. In most electrocatalytic system, the catalyst is supported.^{29,37,40,41} Dispersing the nanoparticle catalysts on a support not only improves the catalytic efficiency of the active component but also promote the even dispersion of the catalysts. This is due to the support's high specific surface area and porous structure, which helps to prevent the aggregation of catalyst nanoparticles, and improves the utilization rate and stability of the catalysts.^{8,24,34,58,70} Furthermore, the support material can act as a co-catalyst, boosting the catalyst's performance through synergistic interactions during the catalytic process.^{30,32,55}

Reactor

Reactor design is crucial to the efficiency of biomass small molecules ECH. An optimized experimental configuration is beneficial for scaling up applications and mitigating mass transfer issues. The design of flow cells and MEAs ensures consistent delivery of biomass small molecules to the working electrode while minimizing mass transfer restrictions caused by hydrogen bubble interference at the electrode surface.^{8,24} The advanced membrane with high ionic conductivity can speed up the rate of ion exchange, thereby reducing the Ohmic resistance within electrolyzers. With the development of Solid-state batteries, the application of solid electrolytes becomes widespread, attributed to their uniform ion-conducting path with lower resistance compared to traditional liquid electrolytes. Polymer ion conductors are suitable for use in ECH processes, outperforming various other solid conductors due to their rapid ion conduction at room temperature, high reliability, and ease of processing.^{71,72} Owing to enhanced mechanical stability and reduced concerns about leakage and evaporation, advanced membrane and solid electrolyte are expected to exhibit superior performance in industrial manufacturing. Reduced Ohmic resistance indicates that a larger current density can be achieved at a given potential.

Table 1. ECH of various biomass molecules in different electrolyzer systems

| Setup | Catalyst | Biomass | Product | Catholyte | Current density (mA cm ⁻²) | FE (%) | Reference |
|----------------|-------------------------------------|------------------------------|---|--|---|--------|---------------------------------|
| H-cell | Ru ₁ Cu | 50 mM HMF | BHMF | 0.5 M PBS | 35 | 89.5 | Ji, K et al. ⁴² |
| H-cell | Ag@CuF | 30 mM HMF | BHMF | PBS | 55 | 45 | Dai, Z et al. ⁵⁵ |
| H-cell | Pd/CF | 50 mM HMF | BHMF | 0.2 M NaClO ₄ | 100 | 50 | Zhang, D et al. ⁴³ |
| H-cell | BiSn | 2 M HMF | BHMF | 0.5 M phosphate | >140 | ~100 | Piao, G et al. ⁶⁰ |
| H-cell | PMo ₁₂ /Cu | 250 mM HMF | BHMF | 0.5 M PBS | ~300 | >70 | Cao, X et al. ⁶¹ |
| H-cell | MoS ₂ -DMA | 35 mM FF | FA | 0.05 M Na ₂ B ₄ O ₇ | 5 | 75 | Tan, J et al. ³⁹ |
| H-cell | Cu _{1.15} /P _{Ag} | 10 mM FF | FA | 1.0 M KOH | 5 | 99 | Wen, H et al. ⁴⁴ |
| H-cell | 15%-Cu/NC ₉₀₀ | 30 mM FF | FA | 1.0 M KOH | 8 | 95 | Xu, W et al. ⁶² |
| H-cell | Cu ₃ N Nw/CuF | 20 mM FF | FA | PBS (pH = 7) | 20 | 83.9 | Wen, H et al. ³⁷ |
| H-cell | ED-Cu | 50 mM FF | FA | 1 M PBS | 100 | 63 | Xia, Z et al. ⁶³ |
| H-cell | ED-Cu | 50 mM FF | FA | 1 M KHCO ₃ | 250 | 93 | Xia, Z et al. ⁶³ |
| H-cell | Cu-CTAB | 50 mM FF | 2-methylfuran (MF) | 0.05 M H ₂ SO ₄ | 200 | 61.3 | Ji, K et al. ³⁶ |
| H-cell | CoS/oms-NSC | 0.2 mM Cinnamaldehyde | Hydrocinnamaldehyde | 1.0 M PBS and acetonitrile (v/v = 4:1) | 12 | 40 | Yuan, X.-S et al. ⁶⁴ |
| H-cell | Rh/CF | 100 mM Cinnamaldehyde | Cinnamic alcohol | 0.2 M NaCl | 50 | 41.15 | Chen, H et al. ⁴¹ |
| H-cell | RhPtRu/CF | 100 mM Guaiacol | Methoxy-cyclohexanes | 0.2 M HClO ₄ | 50 | 62.8 | Wang, M et al. ³⁴ |
| SSER H-cell | Pt/C | 10 mM Diphenyl ether | Cyclohexane/Benzene, Cyclohexanol and Dicyclohexyl ether | 0.25 M PW ₁₂ and 0.68 M NaBH ₄ (80°C) | 25 | 54.9 | Zhai, Q et al. ⁶⁵ |
| SSER H-cell | Pt/C | 10 mM Benzyl phenyl ether | Toluene, Methylcyclohexane, Cyclohexanol and Cyclohexanone | 0.25 M PW ₁₂ and 0.68 M NaBH ₄ (80°C) | 25 | / | Zhai, Q et al. ⁶⁵ |

(Continued on next page)

Table 1. Continued

| Setup | Catalyst | Biomass | Product | Catholyte | Current density (mA cm ⁻²) | FE (%) | Reference |
|---|---------------------|--|---|---|---|--------|-------------------------------------|
| SSER H-cell | Pt/C | 10 mM Phenethoxybenzene | 2-Cyclohexylethanol, Phenol, 2-Cyclohexylethanol and Cyclohexanol, | 0.25 M PW ₁₂ and 0.68 M NaBH ₄ (80°C) | 25 | / | Zhai, Q et al. ⁶⁵ |
| SSER H-cell | Pt/C | 10 mM 4-allyl-2, 6-dimethoxyphenol | Propylcyclohexane and 4-propyl-2, 6-dimethoxycyclohexane | 0.25 M PW ₁₂ and 0.96 M NaBH ₄ (80°C) | 75 | 77.41 | Han, S et al. ⁶⁶ |
| SSER H-cell | Pt/C | 100 mM Phenol | Cyclohexanol and Cyclohexanone | 0.2 M NaCl (50°C) | 109 | 92.39 | Wijaya, Y.P et al. ⁴⁷ |
| SSER H-cell | Pt/C | 100 mM Guaiacol | Cyclohexanol | 0.5 M H ₂ SO ₄ (50°C) | 255 | 37 | Wijaya, Y.P et al. ⁴⁷ |
| SSER H-cell | Pt/C | 89 mM Phenol | Cyclohexanol and Cyclohexane | 0.1 M SiW ₁₂ (35°C) | 800 | 95.3 | Liu, W et al. ⁴⁸ |
| Three-electrode three-compartment cell | Cu-CeO ₂ | 50 mM HMF | BHMF | 0.5 M borate buffer | 23 | 76 | de Luna, G.S et al. ⁴⁰ |
| Membrane reactor | Pd black | 100 mM FF | Methyltetrahydrofuran (MTHF) | t-BuOH | 200 | <17.5 | Stankovic, M.D et al. ⁴⁹ |
| Flow-cell | Ag@CuF | 30 mM HMF | BHMF | PBS (pH7.2–7.4) | 40 | 56.8 | Dai, Z et al. ⁵⁵ |
| Flow-cell | Ag/SnO ₂ | 50 mM HMF | BHMF | 0.5 M KHCO ₃ | 300 | 80.2 | Huang, S et al. ³⁰ |
| Flow-cell | PtRhAu/CF | 120 mM Guaiacol | 2-Methoxycyclohexanol | 0.2 M HClO ₄ | 200 | 58 | Peng, T et al. ⁸ |
| MEA | Pd/VN | 10 mM HMF | 2,5-bishydroxymethyl- tetrahydrofuran (BHMTTHF) | 0.2 M HClO ₄ | 100 | ~36 | Li, S et al. ⁵⁸ |
| MEA | PtNiB/CMK-3 | 10 mM Guaiacol | KA-oil | 0.2 M HClO ₄ | 10 | / | Zhou, Y et al. ⁵⁹ |
| MEA | Rh/CF | 50 mM FA | THFA | 0.2 M HClO ₄ and 30% ethanol | 300 | 54 | Peng, T et al. ²⁴ |
| MEA | Rh/CF | 80 mM Syringol | Methoxy-cyclohexanes | 0.2 M HClO ₄ | 400 | 32 | Peng, T et al. ²⁴ |
| MEA | Rh/CF | 120 mM Guaiacol | Methoxy-cyclohexanes | 0.2 M HClO ₄ | 500 | 44 | Peng, T et al. ²⁴ |

The OER is characterized by its kinetic sluggishness, and the value of the produced O_2 is comparatively low. Integrating the cathodic reduction with an anodic organic oxidation reaction, substituting the OER, facilitates the generation of valuable chemicals.^{29,30,33,55,58} Li et al. coupled the ECH of HMF at the cathode with oxidation of HMF over the CoFeP catalyst (denoted as HMF-ER||HMF-EO). The FE of FDCA over CoFeP are >80% at the potential from 1.73 to 1.93 V (vs. RHE). The voltage the HMF-ER||HMF-EO system needs at 500 mA cm^{-2} is 370 mV lower than that of the HMF-ER||OER system (2.76 V at 500 mA cm^{-2}). This indicates that the HMF-ER||HMF-EO process exhibits superior kinetic favorability.³⁰ Bharath et al. developed a bifunctional catalyst Ru/RGO for ECH and electrooxidation (ECO) of FF. They found the paired electrolyzer achieved a higher MF yield (91%) compared to the MF yield (88%) obtained from the cathodic half-cell reaction. This indicates that anodic H^+ and e^- generated during ECO might have played a role in the ECH of FF, thus contributing to an enhanced selectivity of 2-MF with a high FE of 95%.²⁹ The coupled system outperformed the uncoupled system in terms of added value per unit electric energy generated, suggesting that the integrated coupled system would be beneficial for the valorization of biomass to high-value products.

Electrolyte

In electrolyzers utilizing traditional liquid electrolytes, the reasonable selection of electrolyte is crucial to enhance conductivity, stabilize intermediates, and improve catalyst performance. The kinetics of HER are slower in alkaline media compared to acidic media, attributed to additional water dissociation steps and a more intricate process. However, a catalyst exhibiting good performance in acidic media may show significantly reduced activity in alkaline media.¹¹ The pH and composition of electrolytes can significantly influence the FE and selectivity of ECH.^{44,56} Zou et al. highlighted the proton environment governs the rate of proton-coupled electron transfer (PCET) during hydrogenolysis process and consequently influences the ECH selectivity of FF on Cu electrodes.³⁵ Zhao et al. found that the ECH FE and selectivity of HMF decrease in order of $NaClO_4 > NaCl > Na_2SO_4$, which correlate with the strength of adsorption of the corresponding anions ($SO_4^{2-} > Cl^- > ClO_4^-$) on the Pd surface.⁴³ And when Gyenge et al. substituted acid with weak electrolyte monopotassium phosphate, which has lower conductivity compared to acids, the guaiacol conversion decreased from 85%–91%–0%.⁴⁷ For additives in the electrolytes, Duan et al. reported a strategy to steer selectivity in ECH of FF from producing FA to 2-methylfuran. They used butyl trimethylammonium bromide as a surfactant to modify Cu catalyst, which modulates the electrical double layer. This modification repels interfacial water and weakens the hydrogen-bond (H-bond) network, which is crucial for proton transfer. Therefore, the hydrogen atom transfer (HAT) process is suppressed, consequently inhibiting the conversion of FF to FA.³⁶

And the mixed organic compounds may exhibit the interaction during ECH. Recently, Hou et al. found that phenol enhanced the conversion of benzaldehyde, while benzaldehyde impeded the ECH of phenol. Phenol can enhance the adsorption of benzaldehyde and promotes its conversion on the active site by diminishing the energy barrier required for the reaction.⁷³ Increasing tem-

perature can enhance the *H adsorption within a certain temperature range. Hydrogen desorption takes place simultaneously, competing with the ECH of biomass small molecules. The negative impact of rising temperatures might be attributed to the obstruction of the active site by the reaction substrate adsorbate and accelerated HER.^{65,66} Increased substrate concentrations can lead to enhanced coverage of the catalyst surface by the substrate, promoting an enhancement in ECH.³² However, ECH is constrained by a deficiency in electrocatalytic active sites. Additionally, the overabundance substrate intermediates can result in polymerization reaction, as the inadequate supply of *H prevents it from timely reacting with the excessive intermediates.³⁷

Concurrently, biomass with higher molecular weight exhibits limited water solubility. Lignin is a polymeric macromolecule randomly connected by C–O–C and C–C bonds.⁴ The β -O–4 linkage, the most prevalent in lignin, is particularly promising for research and applications as it can be cleaved with lower energy, thereby maintaining the structural integrity of lignin monomers and their aromatic frameworks, in contrast to the more energetically demanding cleavage of β -1 and β -5 linkages that yield numerous byproducts.¹⁶ Zou et al. depolymerized the β -O–4 linkage through selective C_{aryl} -O(C) bond cleavage, with the CuO nanorod demonstrating a yield of hydroquinone (95.3%) and benzyl alcohol (88.6%).⁷⁴ Nevertheless, the limited solubility of lignin in aqueous media poses a significant constraint on its utilization in electrochemical lignin depolymerization. Although the addition of organic solvent can enhance the solubility, it can lead to restrictions in mass transport and electron transfer, reducing the substrate conversion and electrolyte conductivity. Moreover, the diluted concentration of H^+ , coupled with the competitive occupation of the catalysts' active sites by organic solvents, can decrease the activity of ECH. Additionally, ionic liquid and deep eutectic solvents are employed as electrolytes owing to their superior lignin solubility, broad electrochemical windows and low volatility. However, the high cost and laborious recovery constrain their large-scale application.^{16,54} An electrically conductive organic solvent may thus assume a pivotal role in the ECH of biomass with high concentrations.

CONCLUSIONS AND PERSPECTIVES

ECH of biomass small molecules presents a promising pathway under mild conditions, utilizing green electricity. This review concentrates on the engineering of electrolyzers and available methods of achieving industrial current densities. From the perspective of minimizing Ohmic resistance and increasing mass transport, some modifications, e.g., shorting the distance between electrodes, suspending catalysts in the electrolytes and making the reactor continuous, were applied to improve the performance of ECH of biomass small molecules. Meanwhile, achieve industrial current densities need to consider the intrinsic characteristics of catalysts and supporting materials. The continuous efforts of numerous researchers, supported by abundant green electricity sources, are bringing us closer to large-scale application of this technology. However, achieving industrial-scale production remains a critical challenge.

Currently, only a few studies have attained large current densities (over 100 mA cm⁻²) while maintaining the high FE, high selectivity and high durability.

To advance the industrial production of ECH of biomass small molecules, the primary goal of catalyst development is to ensure the catalytic activity and durability of the catalyst while reducing the catalyst loading and improving the utilization efficiency of metals. Although noble metals have attracted much attention due to their excellent properties, their industrial applications are limited by high cost and scarcity. Therefore, developing low-cost, high-performance catalysts to replace noble metals is crucial. Alloying with non-noble metals not only has significant catalytic effects but also effectively reduces catalyst costs and improves the utilization rate of metals. Both catalysts loaded on a support as working electrode and suspended catalysts can exhibit excellent performance. For the former, despite improvements in the stability of carbon carriers through modification and the development of new materials, many problems persist. For example, carbon support can be corroded, damaging their porous structure and reducing surface area, which causes the catalysts to detach and aggregate, thereby decreasing catalytic activity. Consequently, the development of alternative carriers has significant potential. Suspended catalysts in the electrolyte, characterized by their high specific surface area, effectively overcome kinetic and diffusion challenges posed by reactants and products. This leads to substantial enhancements in both the electrochemical reaction rate and FE, which can be an effective method for achieving industrial-scale current densities.

In ECH processes operating at industrial-scale current densities, the use of flow cells and MEAs, with constantly pumped electrolytes into chambers, ensures a steady supply of biomass small molecules to the catalyst surface. The reduced Ohmic resistance, due to the shorter distance between electrodes, allows the ECH system to improve energy efficiency. However, the stability of current systems does not meet the requirement of thousands of operating hours; the current densities are below the levels needed for amperes, and the handling capacity is insufficient necessary for industrial applications. As the electrolyzer is expanded to an industrial scale, its performance may not increase proportionally, resulting in reduced efficiency, increased costs and increased operational difficulty. Electrodes may not maintain the same activity and stability at larger scales, which may require the development of new electrode materials and designs. The current may be unevenly distributed across the electrode surface, leading to local overheating and reduced electrolysis efficiency. Industrial-grade electrolyzers require integration with upstream feedstock supply and downstream product handling systems, therefore, multistep and cascade reaction reactor will be preferable. The scalability of modular reactor systems can be achieved by the addition of extra modules, enabling an improvement in production capacity without changes in existing infrastructure. Moreover, the modular reactor systems can be customized to optimize the specific ECH process. The modular reactor systems and the integrated strategies combining ECH with conventional approaches can effectively incorporate the ECH into existing industrial settings.

In general, integrated strategies consist of various factors that are essential for achieving good performance at industrial-scale production. Some suggestions are as follows.

- (1) Try to employ non-noble metals and their derivatives as catalysts; efforts can be focused on developing a novel structure material with enhanced catalytic performance through size and morphology optimization, structural modulation, and support regulation. Additionally, explore multifunctional electrocatalysts to ECH the more challenging substrates.
- (2) Compared to the traditional H-cell, the MEA, which operates at lower applied voltages and achieves a high yield, is more applicable for industrial-scale ECH. Try to scale up these fluid electrolyzers to pilot scale production and achieve decentralized production that utilizes the abundant and naturally available wind and solar energy. Moreover, future research should also concentrate on replacing the OER, which exhibits sluggish kinetics and excessive energy consumption, with the valorization of chemicals on anode.
- (3) Factors such as temperature, substrates concentration, electrolyte composition, and the interaction of mixed organic compounds play a role in the ECH process. Adjustments and refinements of these factors are essential for optimizing the ECH performance. Despite ongoing efforts being made to optimize electrolytes, the prevalent approach tends to be mixing aqueous electrolytes with varying proportions of methanol or acetonitrile, aiming to strike a balance between high conductivity, cost-effectiveness, and environmental safety. This underscores the requirement for more rigorous research in this field.

ACKNOWLEDGMENTS

We acknowledge support from the Shenzhen Science and Technology Program (JCYJ20190808150615285).

AUTHOR CONTRIBUTIONS

Y.L. and F.Z. contributed equally. Y.L. wrote the manuscript. F.Z. polished the manuscript. W.B.Z. provided help in manuscript writing. W.Z. supervised this manuscript. All authors commented on the manuscript.

DECLARATION OF INTERESTS

The authors declare no competing interests.

REFERENCES

1. Wang, J., Fu, J., Zhao, Z., Bing, L., Xi, F., Wang, F., Dong, J., Wang, S., Lin, G., Yin, Y., and Hu, Q. (2023). Benefit analysis of multi-approach biomass energy utilization toward carbon neutrality. *Innovations* 4, 100423. <https://doi.org/10.1016/j.xinn.2023.100423>.
2. Wang, Z., Huang, W., Wang, H., Gao, J., Zhang, R., Xu, G., and Wang, Z. (2024). Research on the improvement of carbon neutrality by utilizing agricultural waste: Based on a life cycle assessment of biomass briquette fuel heating system. *J. Clean. Prod.* 434, 140365. <https://doi.org/10.1016/j.jclepro.2023.140365>.
3. Du, W., Cui, Z., Wang, J., Qin, Y., Ye, J., Lin, N., Chen, Y., Duan, W., Chang, Z., Li, H., et al. (2024). Biomass power generation: A pathway to

- carbon neutrality. *Sci. Total. Environ.* 933, 173080. <https://doi.org/10.1016/j.scitotenv.2024.173080>.
- Liu, Y., Nie, Y., Lu, X., Zhang, X., He, H., Pan, F., Zhou, L., Liu, X., Ji, X., and Zhang, S. (2019). Cascade utilization of lignocellulosic biomass to high-value products. *Green Chem.* 21, 3499–3535. <https://doi.org/10.1039/C9GC00473D>.
 - Fu, Q., Xie, W., Yang, L., Yan, L., and Zhao, X. (2024). Recent advances in electrocatalytic upgrading of biomass-derived furfural. *Chem. Eng. J.* 485, 150083. <https://doi.org/10.1016/j.cej.2024.150083>.
 - Aricò, F. (2021). Synthetic approaches to 2,5-bis(hydroxymethyl)furan (BHMF): a stable bio-based diol. *Pure. Appl. Chem.* 93, 551–560. <https://doi.org/10.1515/pac-2021-0117>.
 - Rosatella, A.A., Simeonov, S.P., Frade, R.F.M., and Afonso, C.A.M. (2011). 5-Hydroxymethylfurfural (HMF) as a building block platform: Biological properties, synthesis and synthetic applications. *Green Chem.* 13, 754–793. <https://doi.org/10.1039/C0GC00401D>.
 - Peng, T., Zhuang, T., Yan, Y., Qian, J., Dick, G.R., Behaghel de Bueren, J., Hung, S.-F., Zhang, Y., Wang, Z., Wicks, J., et al. (2021). Ternary Alloys Enable Efficient Production of Methoxylated Chemicals via Selective Electrocatalytic Hydrogenation of Lignin Monomers. *J. Am. Chem. Soc.* 143, 17226–17235. <https://doi.org/10.1021/jacs.1c08348>.
 - Bridgwater, T. (1992). Thermochemical and biochemical biomass conversion activities. *Biomass Bioenergy* 2, 307–318. [https://doi.org/10.1016/0961-9534\(92\)90106-Z](https://doi.org/10.1016/0961-9534(92)90106-Z).
 - Zhang, S., Zou, K., Li, B., Shim, H., and Huang, Y. (2023). Key Considerations on the Industrial Application of Lignocellulosic Biomass Pyrolysis Toward Carbon Neutrality. *Engineering* 29, 35–38. <https://doi.org/10.1016/j.eng.2023.02.015>.
 - Lang, M., and Li, H. (2023). Toward mild synthesis of functional chemicals from lignin-derived phenolics via emerging catalytic technology. *Chem Catal.* 3, 100609. <https://doi.org/10.1016/j.chemcat.2023.100609>.
 - Akhade, S.A., Singh, N., Gutiérrez, O.Y., Lopez-Ruiz, J., Wang, H., Holladay, J.D., Liu, Y., Karkamkar, A., Weber, R.S., Padmaperuma, A.B., et al. (2020). Electrocatalytic Hydrogenation of Biomass-Derived Organics: A Review. *Chem. Rev.* 120, 11370–11419. <https://doi.org/10.1021/acs.chemrev.0c00158>.
 - Carneiro, J., and Nikolla, E. (2019). Electrochemical Conversion of Biomass-Based Oxygenated Compounds. *Annu. Rev. Chem. Biomol. Eng.* 10, 85–104. <https://doi.org/10.1146/annurev-chembioeng-060718-030148>.
 - Lee, J., Cho, H., and Kim, J. (2023). Techno-economic analysis of on-site blue hydrogen production based on vacuum pressure adsorption: Practical application to real-world hydrogen refueling stations. *J. Environ. Chem. Eng.* 11, 109549. <https://doi.org/10.1016/j.jece.2023.109549>.
 - Wang, S., Tarroja, B., Schell, L.S., and Samuelson, S. (2021). Determining cost-optimal approaches for managing excess renewable electricity in decarbonized electricity systems. *Renew. Energy* 178, 1187–1197. <https://doi.org/10.1016/j.renene.2021.06.093>.
 - Yang, C., Chen, H., Peng, T., Liang, B., Zhang, Y., and Zhao, W. (2021). Lignin valorization toward value-added chemicals and fuels via electrocatalysis: A perspective. *Chin. J. Catal.* 42, 1831–1842. [https://doi.org/10.1016/S1872-2067\(21\)63839-1](https://doi.org/10.1016/S1872-2067(21)63839-1).
 - Cheng, S., Zhong, H., and Jin, F. (2023). A mini review of electrocatalytic upgrading of carbohydrate biomass—System, path, and optimization. *Energy Sci. Eng.* 11, 2944–2965. <https://doi.org/10.1002/ese3.1487>.
 - Kundu, B.K., and Sun, Y. (2024). Electricity-driven organic hydrogenation using water as the hydrogen source. *Chem. Sci.* 15, 16424–16435. <https://doi.org/10.1039/D4SC03836C>.
 - Zhang, L., Rao, T.U., Wang, J., Ren, D., Sirisommoonchai, S., Choi, C., Machida, H., Huo, Z., and Norinaga, K. (2022). A review of thermal catalytic and electrochemical hydrogenation approaches for converting biomass-derived compounds to high-value chemicals and fuels. *Fuel Process. Technol.* 226, 107097. <https://doi.org/10.1016/j.fuproc.2021.107097>.
 - Shi, Z., Li, N., Lu, H.-K., Chen, X., Zheng, H., Yuan, Y., and Ye, K.-Y. (2021). Recent advances in the electrochemical hydrogenation of unsaturated hydrocarbons. *Curr. Opin. Electrochem.* 28, 100713. <https://doi.org/10.1016/j.coelec.2021.100713>.
 - Jayan, K., Thadathil, D.A., and Varghese, A. (2023). Electrochemical Hydrogenation of Organic Compounds: A Sustainable Approach. *Asian J. Org. Chem.* 12, e202300309. <https://doi.org/10.1002/ajoc.202300309>.
 - Yang, Q., Ge, B., Yuan, P., Luo, S., Zhang, H., Zhao, Z., Zhang, J., Wang, S., Bao, X., and Yao, X. (2023). Amine Coordinated Electron-Rich Palladium Nanoparticles for Electrochemical Hydrogenation of Benzaldehyde. *Adv. Funct. Mater.* 33, 2214588. <https://doi.org/10.1002/adfm.202214588>.
 - Kleinhaus, J.T., Wolf, J., Pellumbi, K., Wickert, L., Viswanathan, S.C., Junge Puring, K., Siegmund, D., and Apfel, U.-P. (2023). Developing electrochemical hydrogenation towards industrial application. *Chem. Soc. Rev.* 52, 7305–7332. <https://doi.org/10.1039/D3CS00419H>.
 - Peng, T., Zhang, W., Liang, B., Lian, G., Zhang, Y., and Zhao, W. (2023). Electrocatalytic valorization of lignocellulose-derived aromatics at industrial-scale current densities. *Nat. Commun.* 14, 7229. <https://doi.org/10.1038/s41467-023-43136-y>.
 - Leow, W.R., Lum, Y., Ozden, A., Wang, Y., Nam, D.-H., Chen, B., Wicks, J., Zhuang, T.-T., Li, F., Sinton, D., and Sargent, E.H. (2020). Chloride-mediated selective electrosynthesis of ethylene and propylene oxides at high current density. *Science* 368, 1228–1233. <https://doi.org/10.1126/science.aaz8459>.
 - Franke, M.C., Longley, V.R., Rafiee, M., Stahl, S.S., Hansen, E.C., and Weix, D.J. (2022). Zinc-free, Scalable Reductive Cross-Electrophile Coupling Driven by Electrochemistry in an Undivided Cell. *ACS Catal.* 12, 12617–12626. <https://doi.org/10.1021/acscatal.2c03033>.
 - Qiu, H., Shuai, B., Wang, Y.-Z., Liu, D., Chen, Y.-G., Gao, P.-S., Ma, H.-X., Chen, S., and Mei, T.-S. (2020). Enantioselective Ni-Catalyzed Electrochemical Synthesis of Biaryl Atropisomers. *J. Am. Chem. Soc.* 142, 9872–9878. <https://doi.org/10.1021/jacs.9b13117>.
 - Park, K., Pintauro, P.N., Baizer, M.M., and Nobe, K. (1986). Current efficiencies and regeneration of poisoned raney nickel in the electrohydrogenation of glucose to sorbitol. *J. Appl. Electrochem.* 16, 941–946. <https://doi.org/10.1007/bf01006542>.
 - Bharath, G., and Banat, F. (2021). High-Grade Biofuel Synthesis from Paired Electrohydrogenation and Electrooxidation of Furfural Using Symmetric Ru/Reduced Graphene Oxide Electrodes. *ACS Appl. Mater. Interfaces* 13, 24643–24653. <https://doi.org/10.1021/acsaami.1c02231>.
 - Guo, X., Fu, H., Yang, J., Luo, L., Zhou, H., Xu, M., Kong, X., Shao, M., Duan, H., and Li, Z. (2023). Promoting Electrocatalytic Hydrogenation of 5-Hydroxymethylfurfural over a Cooperative Ag/SnO₂ Catalyst in a Wide Potential Window. *ACS Catal.* 13, 13528–13539. <https://doi.org/10.1021/acscatal.3c03005>.
 - Huang, S., Gong, B., Jin, Y., Sit, P.H.L., and Lam, J.C.-H. (2022). The Structural Phase Effect of MoS₂ in Controlling the Reaction Selectivity between Electrocatalytic Hydrogenation and Dimerization of Furfural. *ACS Catal.* 12, 11340–11354. <https://doi.org/10.1021/acscatal.2c02137>.
 - Garedew, M., Young-Farhat, D., Jackson, J.E., and Saffron, C.M. (2019). Electrocatalytic Upgrading of Phenolic Compounds Observed after Lignin Pyrolysis. *ACS Sustain. Chem. Eng.* 7, 8375–8386. <https://doi.org/10.1021/acssuschemeng.9b00019>.
 - Li, X., Cong, L., Wu, Y., Lin, N., Liu, F., Xin, D., Han, F., Yang, J., Chen, W., and Lin, H. (2023). Strategies for controlling gas evolution reactions to boost the divergent paired electrochemical upgrading of furfural in acidic environment. *Chem. Eng. J.* 470, 144093. <https://doi.org/10.1016/j.cej.2023.144093>.
 - Wang, M., Peng, T., Yang, C., Liang, B., Chen, H., Kumar, M., Zhang, Y., and Zhao, W. (2022). Electrocatalytic hydrogenation of lignin monomer to methoxy-cyclohexanes with high faradaic efficiency. *Green Chem.* 24, 142–146. <https://doi.org/10.1039/d1gc03523a>.

35. Zhou, L., Li, Y., Lu, Y., Wang, S., and Zou, Y. (2022). pH-Induced selective electrocatalytic hydrogenation of furfural on Cu electrodes. *Chin. J. Catal.* **43**, 3142–3153. [https://doi.org/10.1016/S1872-2067\(22\)64119-6](https://doi.org/10.1016/S1872-2067(22)64119-6).
36. Ji, K., Liu, Y., Wang, Y., Kong, K., Li, J., Liu, X., and Duan, H. (2024). Steering Selectivity in Electrocatalytic Furfural Reduction via Electrode–Electrolyte Interface Modification. *J. Am. Chem. Soc.* **146**, 11876–11886. <https://doi.org/10.1021/jacs.4c00818>.
37. Wen, H., Li, T., Fan, Z., Jing, Y., Zhang, W., and Chen, Z. (2024). Electrocatalytic hydrogenation of furfural over copper nitride with enhanced hydrogen spillover performance. *Green Chem.* **26**, 8861–8871. <https://doi.org/10.1039/d4gc01868k>.
38. Xia, Z., Li, Y., Wu, J., Huang, Y.-C., Zhao, W., Lu, Y., Pan, Y., Yue, X., Wang, Y., Dong, C.-L., et al. (2022). Promoting the electrochemical hydrogenation of furfural by synergistic Cu₀–Cu⁺ active sites. *Sci. China Chem.* **65**, 2588–2595. <https://doi.org/10.1007/s11426-022-1407-0>.
39. Tan, J., Zhang, W., Shu, Y., Lu, H., Tang, Y., and Gao, Q. (2021). Interlayer engineering of molybdenum disulfide toward efficient electrocatalytic hydrogenation. *Sci. Bull.* **66**, 1003–1012. <https://doi.org/10.1016/j.scib.2020.11.002>.
40. de Luna, G.S., Zeller, P., Öztuna, E., Maluta, F., Canciani, A., Ospitali, F., Ho, P.H., Paglianti, A., Knop-Gericke, A., Fornasari, G., et al. (2023). In Situ Development of a 3D Cu–CeO₂ Catalyst Selective in the Electrocatalytic Hydrogenation of Biomass Furanic Compounds. *ACS Catal.* **13**, 12737–12745. <https://doi.org/10.1021/acscatal.3c03363>.
41. Chen, H., Peng, T., Liang, B., Zhang, D., Lian, G., Yang, C., Zhang, Y., and Zhao, W. (2022). Efficient electrocatalytic hydrogenation of cinnamaldehyde to value-added chemicals. *Green Chem.* **24**, 3655–3661. <https://doi.org/10.1039/d1gc04777a>.
42. Ji, K., Xu, M., Xu, S.-M., Wang, Y., Ge, R., Hu, X., Sun, X., and Duan, H. (2022). Electrocatalytic Hydrogenation of 5-Hydroxymethylfurfural Promoted by a Ru₁Cu Single-Atom Alloy Catalyst. *Angew. Chem. Int. Ed. Engl.* **61**, e202209849. <https://doi.org/10.1002/anie.202209849>.
43. Zhang, D., Lian, G., Zhang, W., Mo, Z., Chen, H., Liang, B., Zhang, Y., and Zhao, W. (2023). Selective electrocatalytic hydrogenation of lignocellulose-derived 5-hydroxymethylfurfural with superior productivities. *iScience* **26**, 108003. <https://doi.org/10.1016/j.isci.2023.108003>.
44. Wen, H., Fan, Z., Dou, S., Lam, J.C.-H., Zhang, W., and Chen, Z. (2024). Electrochemical hydrogenation of furfural under alkaline conditions with enhanced furfuryl alcohol selectivity by self-grown Cu on a Ag electrode. *Inorg. Chem. Front.* **11**, 4449–4458. <https://doi.org/10.1039/d4qi00763h>.
45. Zhou, P., Chen, Y., Luan, P., Zhang, X., Yuan, Z., Guo, S.-X., Gu, Q., Johannessen, B., Mollah, M., Chaffee, A.L., et al. (2021). Selective electrochemical hydrogenation of furfural to 2-methylfuran over a single atom Cu catalyst under mild pH conditions. *Green Chem.* **23**, 3028–3038. <https://doi.org/10.1039/d0gc03999c>.
46. Song, Y., Chia, S.H., Sanyal, U., Gutiérrez, O.Y., and Lercher, J.A. (2016). Integrated catalytic and electrocatalytic conversion of substituted phenols and diaryl ethers. *J. Catal.* **344**, 263–272. <https://doi.org/10.1016/j.jcat.2016.09.030>.
47. Wijaya, Y.P., Grossmann-Neuhausler, T., Dhewangga Putra, R.D., Smith, K.J., Kim, C.S., and Gyenge, E.L. (2020). Electrocatalytic Hydrogenation of Guaiacol in Diverse Electrolytes Using a Stirred Slurry Reactor. *ChemSusChem* **13**, 629–639. <https://doi.org/10.1002/cssc.201902611>.
48. Liu, W., You, W., Gong, Y., and Deng, Y. (2020). High-efficiency electrochemical hydrodeoxygenation of bio-phenols to hydrocarbon fuels by a superacid-noble metal particle dual-catalyst system. *Energy Environ. Sci.* **13**, 917–927. <https://doi.org/10.1039/c9ee02783a>.
49. Stankovic, M.D., Sperry, J.F., Delima, R.S., Rupnow, C.C., Rooney, M.B., Stolar, M., and Berlinguette, C.P. (2023). Electrochemical production of methyltetrahydrofuran, a biofuel for diesel engines. *Energy Environ. Sci.* **16**, 3453–3461. <https://doi.org/10.1039/d3ee01079a>.
50. Wijaya, Y.P., Smith, K.J., Kim, C.S., and Gyenge, E.L. (2020). Electrocatalytic hydrogenation and depolymerization pathways for lignin valorization: toward mild synthesis of chemicals and fuels from biomass. *Green Chem.* **22**, 7233–7264. <https://doi.org/10.1039/d0gc02782k>.
51. He, Z.-D., Chen, Y.-X., Santos, E., and Schmickler, W. (2018). The Pre-exponential Factor in Electrochemistry. *Angew. Chem., Int. Ed. Engl.* **57**, 7948–7956. <https://doi.org/10.1002/anie.201800130>.
52. Wijaya, Y.P., Putra, R.D.D., Smith, K.J., Kim, C.S., and Gyenge, E.L. (2021). Guaiacol Hydrogenation in Methanesulfonic Acid Using a Stirred Slurry Electrocatalytic Reactor: Mass Transport and Reaction Kinetics Aspects. *ACS Sustain. Chem. Eng.* **9**, 13164–13175. <https://doi.org/10.1021/acssuschemeng.1c03332>.
53. Wijaya, Y.P., Smith, K.J., Kim, C.S., and Gyenge, E.L. (2021). Synergistic effects between electrocatalyst and electrolyte in the electrocatalytic reduction of lignin model compounds in a stirred slurry reactor. *J. Appl. Electrochem.* **51**, 51–63. <https://doi.org/10.1007/s10800-020-01429-w>.
54. Chen, G., Liang, L., Li, N., Lu, X., Yan, B., and Cheng, Z. (2021). Upgrading of Bio-Oil Model Compounds and Bio-Crude into Biofuel by Electrocatalysis: A Review. *ChemSusChem* **14**, 1037–1052. <https://doi.org/10.1002/cssc.202002063>.
55. Dai, Z., Liu, X., Liu, N., Zhang, Y., and Zhao, X. (2024). Upgrading biomass derived furan aldehydes by coupled electrochemical conversion over silver-based electrocatalysts. *Chem. Eng. J.* **488**, 151001. <https://doi.org/10.1016/j.cej.2024.151001>.
56. Zhang, Y., and Shen, Y. (2024). Electrochemical hydrogenation of levulinic acid, furfural and 5-hydroxymethylfurfural. *Appl. Catal. B Environ.* **343**, 123576. <https://doi.org/10.1016/j.apcatb.2023.123576>.
57. O'Brien, C.P., Miao, R.K., Shayesteh Zeraati, A., Lee, G., Sargent, E.H., and Sinton, D. (2024). CO₂ Electrolyzers. *Chem. Rev.* **124**, 3648–3693. <https://doi.org/10.1021/acs.chemrev.3c00206>.
58. Li, S., Sun, X., Yao, Z., Zhong, X., Cao, Y., Liang, Y., Wei, Z., Deng, S., Zhuang, G., Li, X., and Wang, J. (2019). Biomass Valorization via Paired Electrosynthesis Over Vanadium Nitride-Based Electrocatalysts. *Adv. Funct. Mater.* **29**, 1904780. <https://doi.org/10.1002/adfm.201904780>.
59. Zhou, Y., Gao, Y., Zhong, X., Jiang, W., Liang, Y., Niu, P., Li, M., Zhuang, G., Li, X., and Wang, J. (2019). Electrocatalytic Upgrading of Lignin-Derived Bio-Oil Based on Surface-Engineered PtNiB Nanostructure. *Adv. Funct. Mater.* **29**, 1807651. <https://doi.org/10.1002/adfm.201807651>.
60. Piao, G., Yoon, S.H., Cha, H.G., Han, D.S., and Park, H. (2022). Porous dendritic BiSn electrocatalysts for hydrogenation of 5-hydroxymethylfurfural. *J. Mater. Chem. A Mater.* **10**, 24006–24017. <https://doi.org/10.1039/d2ta05969j>.
61. Cao, X., Ding, Y., Chen, D., Ye, W., Yang, W., and Sun, L. (2024). Cluster-Level Heterostructure of PMo₁₂/Cu for Efficient and Selective Electrocatalytic Hydrogenation of High-Concentration 5-Hydroxymethylfurfural. *J. Am. Chem. Soc.* **146**, 25125–25136. <https://doi.org/10.1021/jacs.4c08205>.
62. Xu, W., Yu, C., Chen, J., and Liu, Z. (2022). Electrochemical hydrogenation of biomass-based furfural in aqueous media by Cu catalyst supported on N-doped hierarchically porous carbon. *Appl. Catal. B Environ.* **305**, 121062. <https://doi.org/10.1016/j.apcatb.2022.121062>.
63. Xia, Z., Xu, L., Ma, C., An, Q., Bu, C., Fan, Y., Lu, Y., Pan, Y., Xie, D., Liu, Q., et al. (2024). Enhancing the Electrocatalytic Hydrogenation of Furfural via Anion-Induced Molecular Activation and Adsorption. *J. Am. Chem. Soc.* **146**, 24570–24579. <https://doi.org/10.1021/jacs.4c07979>.
64. Yuan, X.-S., Zhou, S.-H., Wang, S.-M., Wei, W., Li, X., Wu, X.-T., and Zhu, Q.-L. (2025). Ordered macroporous superstructure of defective carbon adorned with tiny cobalt sulfide for selective electrocatalytic hydrogenation of cinnamaldehyde. *Appl. Catal., B: Environment and Energy* **361**, 124642. <https://doi.org/10.1016/j.apcatb.2024.124642>.
65. Zhai, Q., Han, S., Wang, K., Jiang, J., and Xu, J. (2022). Electrocatalytic cleavage of aryl ether C–O linkages in lignin model dimers. *Fuel Process. Technol.* **235**, 107350. <https://doi.org/10.1016/j.fuproc.2022.107350>.
66. Han, S., Zhang, X., Wang, R., Wang, K., Jiang, J., and Xu, J. (2023). Electrocatalytic conversion of G-type and S-type phenolic compounds from

- different tree species in a heteropolyacid fluidized system. *Chem. Eng. J.* **452**, 139299. <https://doi.org/10.1016/j.cej.2022.139299>.
67. Seh, Z.W., Kibsgaard, J., Dickens, C.F., Chorkendorff, I., Nørskov, J.K., and Jaramillo, T.F. (2017). Combining theory and experiment in electrocatalysis: Insights into materials design. *Science* **355**, eaad4998. <https://doi.org/10.1126/science.aad4998>.
 68. Zeng, Y., Zhao, M., Zeng, H., Jiang, Q., Ming, F., Xi, K., Wang, Z., and Liang, H. (2023). Recent progress in advanced catalysts for electrocatalytic hydrogenation of organics in aqueous conditions. *eScience* **3**, 100156. <https://doi.org/10.1016/j.esci.2023.100156>.
 69. Zhou, L., Zhu, X., Su, H., Lin, H., Lyu, Y., Zhao, X., Chen, C., Zhang, N., Xie, C., Li, Y., et al. (2021). Identification of the hydrogen utilization pathway for the electrocatalytic hydrogenation of phenol. *Sci. China Chem.* **64**, 1586–1595. <https://doi.org/10.1007/s11426-021-1100-y>.
 70. Wang, Y., Cui, X., Zhang, J., Qiao, J., Huang, H., Shi, J., and Wang, G. (2022). Advances of atomically dispersed catalysts from single-atom to clusters in energy storage and conversion applications. *Prog. Mater. Sci.* **128**, 100964. <https://doi.org/10.1016/j.pmatsci.2022.100964>.
 71. Xia, C., Zhu, P., Jiang, Q., Pan, Y., Liang, W., Stavitski, E., Alshareef, H.N., and Wang, H. (2019). Continuous production of pure liquid fuel solutions via electrocatalytic CO₂ reduction using solid-electrolyte devices. *Nat. Energy* **4**, 776–785. <https://doi.org/10.1038/s41560-019-0451-x>.
 72. Xia, C., Xia, Y., Zhu, P., Fan, L., and Wang, H. (2019). Direct electrosynthesis of pure aqueous H₂O₂ solutions up to 20% by weight using a solid electrolyte. *Science* **366**, 226–231. <https://doi.org/10.1126/science.aay1844>.
 73. Liang, L., Wang, C., Lu, X., Sun, Y., Yan, B., Li, N., Chen, G., and Hou, L. (2024). Interactions of phenol and benzaldehyde in electrocatalytic upgrading process. *Chin. Chem. Lett.* **35**, 108581. <https://doi.org/10.1016/j.ccllet.2023.108581>.
 74. He, Y., Zeng, X., Lu, Z., Mo, S., An, Q., Liu, Q., Yang, Y., Lan, W., Wang, S., and Zou, Y. (2024). Aqueous Electrocatalytic Hydrogenation Depolymerization of Lignin β-O-4 Linkage via Selective Caryl–O(C) Bond Cleavage: The Regulation of Adsorption. *J. Am. Chem. Soc.* **146**, 32022–32031. <https://doi.org/10.1021/jacs.4c12220>.